CEO Clinical and Experimental Otorhinolaryngology Vol. 4, No. 1: 18-23, March 2011 DOI 10.3342/ceo.2011.4.1.18

Original Article

Decreased Immunoreactivities and Functions of the Chloride Transporters, KCC2 and NKCC1, in the Lateral Superior Olive Neurons of Circling Mice

Jonu Pradhan, BS · Dhiraj Maskey, PhD[1] · Ki Sup Park, MS[1] · Myeung Ju Kim, MD[1] · Seung Cheol Ahn, MD[2]

Departments of Nanobio Medical Science,[1] Anatomy, and [2] Physiology, Dankook University College of Medicine, Cheonan, Korea

Objectives. We tested the possibility of differential expression and function of the potassium-chloride (KCC2) and sodium-potassium-2 chloride (NKCC1) co-transporters in the lateral superior olive (LSO) of heterozygous (+/*cir*) or homozygous (*cir*/*cir*) mice.

Methods. Mice pups aged from postnatal (P) day 9 to 16 were used. Tails from mice were cut for DNA typing. For Immunohistochemical analysis, rabbit polyclonal anti-KCC2 or rabbit polyclonal anti-NKCC1 was used and the density of immunolabelings was evaluated using the NIH image program. For functional analysis, whole cell voltage clamp technique was used in brain stem slices and the changes of reversal potentials were evaluated at various membrane potentials.

Results. Immunohistochemical analysis revealed both KCC2 and NKCC1 immunoreactivities were more prominent in heterozygous (+/*cir*) than homozygous (*cir*/*cir*) mice on P day 16. In P9–P12 heterozygous (+/*cir*) mice, the reversal potential (E_{gly}) of glycine-induced currents was shifted to a more negative potential by 50 μM bumetanide, a known NKCC1 blocker, and the negatively shifted E_{gly} was restored by additional application of 1 mM furosemide, a KCC2 blocker (-58.9±2.6 mV to -66.0±1.5 mV [bumetanide], -66.0±1.5 mV to -59.8±2.8 mV [furosemide+bumetanide], n=11). However, only bumetanide was weakly, but significantly effective (-60.1±2.9 mV to -62.7±2.6 mV [bumetanide], -62.7±2.6 mV to -62.1±2.5 mV [furosemide+bumetanide], n=7) in P9–P12 homozygous (*cir*/*cir*) mice.

Conclusion. The less prominent immunoreactivities and weak or absent responses to bumetanide or furosemide suggest impaired function or delayed development of both transporters in homozygous (*cir*/*cir*) mice.

Key Words. *Potassium-chloride co-transporter, Sodium-potassium-2 chloride co-transporter, Lateral superior olive, Circling mice*

INTRODUCTION

The circling mouse is a recently developed animal model for human non-syndromic hearing loss (DFNB6), which is inherited in an autosomal recessive mode with 100% penetrance (1-3). The deafness is caused by spontaneous degeneration of cochlear hair cells, which is completed as early as postnatal (P) day 21 (1). The abnormal changes are not limited to the cochlea. We have reported that in the auditory brain stem, the developing medial nucleus of trapezoid body (MNTB) – lateral superior olive (LSO) synapses, which are gamma-aminobutyric acid (GABA)/glycine/glutamatergic synapses at birth and become inhibitory glycinergic synapses after the onset of hearing in rats (4), have glutamate as a major neurotransmitter instead of glycine immediately after birth, and glutamatergic transmission is sustained at a later period (P9-P11) of synapse development in homozygous (*cir*/*cir*) circling mice (5).

• Received July 28, 2010
Accepted after revision September 27, 2010

• Corresponding author: **Seung Cheol Ahn, MD**
Department of Physiology, Dankook University College of Medicine,
San 29 Anseo-dong, Cheonan 330-714, Korea
Tel: +82-41-550-3852, Fax: +82-41-565-6167
E-mail: ansil67@hanmail.net

Like other immature neuronal systems (6-10), the developing MNTB-LSO synapses in rats undergo a depolarizing-hyperpolarizing shift (11, 12), which depends on the changes of Cl^- reversal potentials relative to resting membrane potentials, and is mainly caused by temporal changes in the internal concentration of Cl^- ($[Cl^-]_{in}$) of LSO neurons. Two cation-chloride co-transporters, potassium-chloride co-transporter 2 (KCC2) and sodium-potassium-2 chloride co-transporter 1 (NKCC1), are major candidates for the changes of $[Cl^-]_{in}$ in developing neurons (13, 14).

The developing MNTB-LSO synapses of circling mice have two characteristic features. One is the enhanced glutamatergic transmission and the other is the underdevelopment of glycine receptors of LSO neurons (5). These two factors might play a certain role in the development of Cl^- transporters. Indeed, it has been suggested that Ca^{2+} influx through N-methyl-D-aspartate (NMDA) receptors is a cause of down-regulation of KCC2 in dissociated cultures of mature hippocampal neurons (15), and LSO neurons isolated from strychnine-reared rats at P14–P16 have a relatively high $[Cl^-]_{in}$ compared to neurons from control rats (16). Moreover, neuronal circuit activity has been suggested to affect the function or expression of KCC2 (17) and bilateral cochlear ablation before hearing onset has been reported to abolish the expression of KCC2 mRNA in P14-P15 rat LSO (16). In the inferior colliculus of gerbils, bilateral cochlear ablation before the onset of hearing also reduces the ability of neurons to transport Cl^-, although the levels of NKCC1 and KCC2 mRNA are unchanged (18). Taken together, these reports raise the possibility of abnormal development and/or function of Cl^- transporters in homozygous (*cir/cir*) mice, in which the cochlea begins to degenerate spontaneously after birth and GABA/glycinergic inputs are weak in MNTB-LSO synapses. Thus, we investigated the alterations of KCC2 and NKCC1 expression in neonatal circling mice using immunohistochemistry and whole cell voltage clamp technique.

MATERIALS AND METHODS

The data presented herein were obtained from pups between P9-P16. Tails from mice were cut for DNA typing. The detailed preparation procedure has been described in our previous report (5). The animals were maintained in the Animal Facility of Dankook University, and the Dankook University Institutional Animal Care and Use Committee (DUIAC) approved this study. For electrophysiological studies, 300-μm thick coronal slices were cut with a vibratome (LEICA VT1000s, LEICA Microsystems, Heidelberg, Germany). The slices were transferred to a submersion-type chamber mounted on an upright microscope and perfused continuously with aCSF containing the following (in mM): NaCl (124), KCl (5), KH_2PO_4 (1.25), glucose (10), $NaHCO_3$ (26), $CaCl_2$ (2), $MgSO_4$ (1.3), and kynurenic acid (1). We used the whole cell voltage clamp technique and analyzed the data according to the methods described by DeFazio et al. (19). The membrane potential was stepped from -100 to -30–-40 mV with increments of 10 mV and glycine puffs during the voltage steps elicited transient currents (Fig. 1A). The recording electrodes (2–3 MΩ) were filled with solution containing the following (in mM): K-gluconate (128.4), EGTA (5), KCl (4.6), hydroxyethylpiperazine-N-2-ethanesulfonic acid (HEPES) (10), Na_2GTP (0.2), MgATP (2), KOH (20), $CaCl_2$ (0.2), and QX 314 (5). Series resistance (R_s) was not compensated, but monitored by the application of a small depolarizing pulse in every trial. Only recordings with a stable R_s (<20 MΩ or <25% change in R_s) were used in the analysis. The calculated junction potentials and voltage errors produced by the R_s and glycine induced-currents were subtracted from commanding potentials to produce the real voltages applied. The junction potential was calculated using software (Clampex 9.0, Molecular Devices, Sunnyvale, CA, USA). These corrected voltages were used to plot the currents induced by pressure application of glycine (Fig. 1B, C).

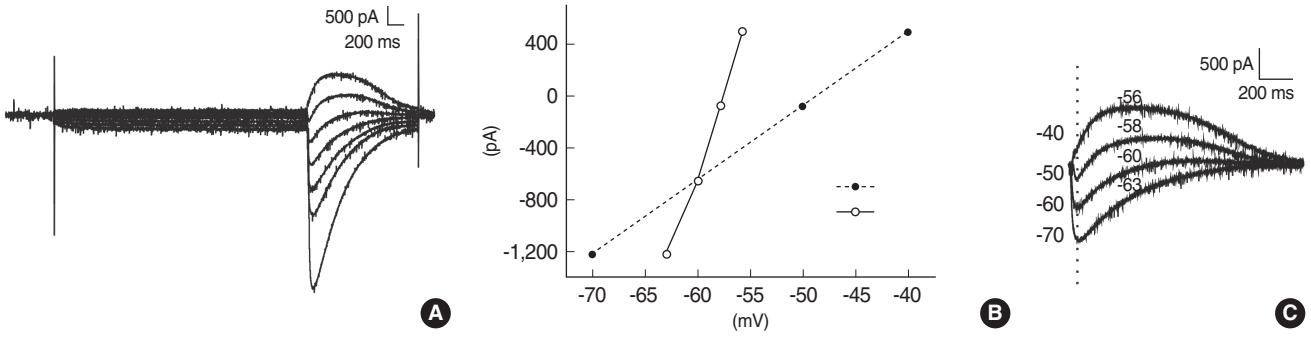

Fig. 1. The reversal potential of the glycine-evoked currents measured from the amplitudes of the responses at different step potentials. Glycine puffs during the voltage steps from -100 mV to -40 mV with increments of 10 mV elicited transient currents (A). In (C), the baseline current at each step potential was subtracted from the raw traces shown in (A). The amplitude of the currents at the vertical dotted line in (C) was plotted as a function of applied potentials (B). Filled circles represent the amplitudes as a function of the command potential, while hollow circles represent the amplitudes as a function of the corrected potential. The corrected potentials (-56, -58, -60, and -63) at given commanding potentials (-40, -50, -60, and -70) are present in (C).

Pressure application was controlled by a Toohey Spritzer pressure system IIe (Toohey Company, Fairfield, NJ, USA). Pressure pulses of 20 ms were delivered at 5–10 psi. More than three consecutive data points close to zero current were selected for a linear fit to calculate the reversal potential of glycine (E_{gly}) using the Nernst equation ($E_{gly}=59.16\times\log_{10}([Cl]_{in}/[Cl]_{out})$ (at 25ºC).

All chemicals, except QX 314 (Tocris), were purchased from Sigma. The data were filtered at 5 kHz (EPC-8, HEKA, Freiburg, Germany), digitized at 10 kHz, and stored on a computer using a homemade program (R-clamp 1.23). The analysis of the electrophysiologic data and statistical testing were performed with Clampfit 9.2 (Molecular Devices) and Origin 7.0 (OriginLab Corporation, Northampton, MA, USA). Data are expressed as the mean±standard error of the mean throughout the text. Comparisons were made using the Student's *t*-test, and a *P*-value<0.05 was considered as statistically significant.

Immunohistochemical staining was performed, as described earlier (5). Briefly, after washing with phosphate buffered saline (PBS), treatment with 1% H_2O_2 was followed by incubation for 48 hours at 4ºC with rabbit polyclonal anti-KCC2 (07-432, Millipore, Temecula, CA, USA) or rabbit polyclonal anti-NKCC1 (AB59791, Abcam, Cambridge, UK) in blocking buffer (2% bovine serum albumin, 0.3% Triton X-100, 1% horse serum, and 0.1 M PBS). The dilution ratios of KCC2 and NKCC1 at P16 were 1:70,000 and 1:2,000, respectively. The sections were evaluated using an Olympus BX51 microscope and photographs of the sections were obtained with a microscope digital camera system (DP50, Tokyo, Olympus, Japan). The NIH image program (Scion Image) was used to determine the staining densities.

RESULTS

As NKCC1 develops late (around P12) compared to KCC2 in rats (20), we investigated the immunohistochemistry of KCC2 and NKCC1 in LSO neurons of heterozygous (+/*cir*) and homozygous (*cir*/*cir*) mice on P16. On P16, KCC2 immunoreactivities were observed in the LSO of both heterozygous (+/*cir*) and homozygous (*cir*/*cir*) mice (Fig. 2A, B). The labeling signals were closely related to the plasma membrane in both groups (Fig. 2C, D). KCC2 immunoreactivities of heterozygous (+/*cir*) mice were more prominent than homozygous (*cir*/*cir*) mice in LSO. The mean densities of KCC2 on P16 were 92.1±2.7 mm^{-2} (heterozygous) and 82.2±4.1 mm^{-2} (homozygous) in 15 paired slic-

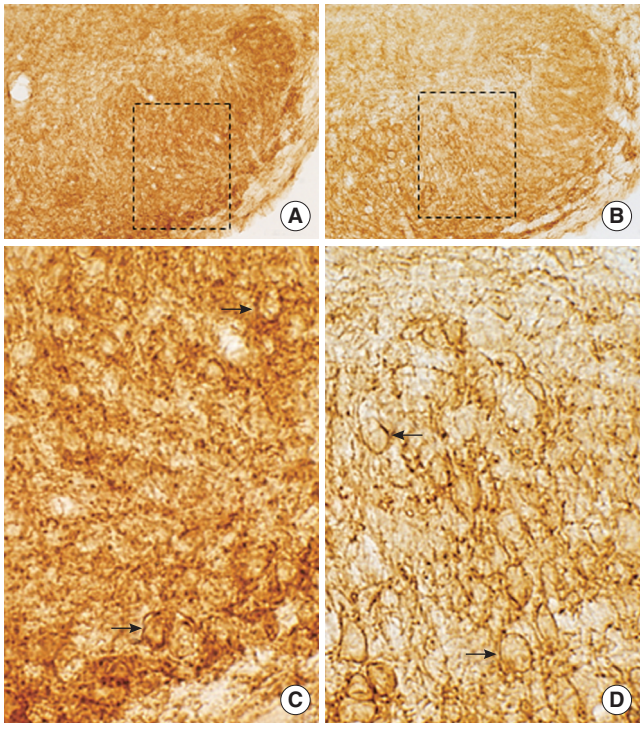

Fig. 2. The localization of potassium-chloride co-transporter 2 (KCC2) immunoreactivity (IR) in lateral superior olive (LSO) of heterozygous (+/*cir*) (A, C) and homozygous (*cir*/*cir*) mice (B, D). At P16, KCC2 immunoreactivities were observed in LSO of both genotypes (A, B). The selected areas (dashed-line box) in A and B are magnified in C and D, respectively. The arrows indicate KCC2 immunoreactivity confined to the cell membrane (C, D). Scale bars=200 μm in A, B; 50 μm in C, D.

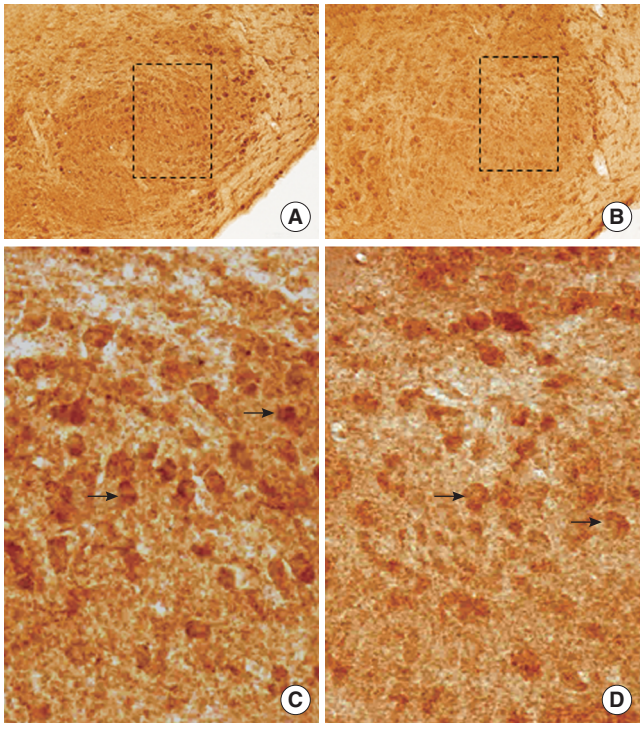

Fig. 3. The localization of sodium-potassium-2 chloride co-transporter 1 (NKCC1) IR in the lateral superior olive (LSO) of heterozygous (+/*cir*) (A, C) and homozygous (*cir*/*cir*) mice (B, D). On P16, NKKC1 immunoreactivities were observed in LSO of both genotypes (A, B). The selected areas (dashed-line box) in A and B are magnified in C and D, respectively. The arrows indicate NKCC1 immunoreactivities (C, D). Scale bars=200 μm in A, B; 50 μm in C, D.

es. The two values were significantly different. We also found the more prominent immunoreactivities of NKCC1 in heterozygous (+/*cir*) mice than in homozygous (*cir/cir*) mice (Fig. 3A, B). The LSO neurons of heterozygous (+/*cir*) mice were more darkly stained than homozygous (*cir/cir*) mice (Fig. 3C, D). The mean densitites of NKCCl immunoreactivities were 118.72±3.27 mm^{-2} (heterozygous) and 109.06±1.08 mm^{-2} (homozygous) on P16.

To investigate the functional aspect of transporters, we used the whole cell voltage clamp technique in P9–P12 mice. The calculated E_{gly} of glycine currents from linear fits were -58.9±2.6 mV (n=11) in heterozygous (+/*cir*) mice and -60.1±2.9 mV (n=7) in homozygous (*cir/cir*) mice. These two values were not significantly different. To elucidate the involvement of NKCC1, 50 μM bumetanide, a known selective blocker of NKCC1 (21), was perfused and glycine-induced currents were recorded again after a 20 minutes perfusion of bumetanide at various potentials. In heterozygous (+/*cir*) mice, the mean E_{gly} shifted significantly to a more negative potential from -58.9±2.6 mV to -66.0±1.5 mV (paired *t*-test, $P<0.05$, n=11) (Fig. 4A, B) by 50 μM bumetanide. In homozygous (*cir/cir*) mice, 50 μM bumetanide also shifted the control E_{gly} (-60.1±2.9 mV) weakly, but significantly to a more negative potential (-62.7±2.6 mV, paired *t*-test, $P<0.05$, n=7) (Fig. 4C, D). We tested the involvement of KCC2 in the determination of E_{gly} using 1 mM furosemide, the concentration of which is known to block KCC2 completely (22). We reasoned that if KCC2 worked antagonistically to NKCC1, an additional application of furosemide combined with bumetanide would shift the E_{gly} to a less negative potential in heterozygous (+/*cir*) or homozygous (*cir/cir*) mice. Additional perfusion of 50 μM bumetanide with 1 mM furosemide significantly changed the E_{gly} recorded in the bumetanide-only condition in heterozygous (+/*cir*) mice (-66.0±1.5 mV to -59.8±2.8 mV, n=11) (Fig. 4A, B), while in homozygous (*cir/cir*) mice, E_{gly} recorded in the presence of bumetanide alone did not recover by the successive application of 1 mM furosemide with 50 μM bumetanide (-62.7±2.6 mV to -62.1±2.5 mV, n=7) (Fig. 4C , D).

DISCUSSION

At P9–P12, the E_{gly}s recorded with the whole cell configuration were relatively less negative (-58.9 mV [heterozygous {+/*cir*}], -60.1 mV [homozygous {*cir/cir*}]) compared to the theoretical value (-84.3 mV), implying the existence of some Cl^- accumulation mechanisms in both genotypes. One of the mechanisms might be NKCC1, the thermodynamic driving force of which favors Cl- accumulation over the range of the physiologic concentration of $[Cl^-]_{in}$ and $[K^+]_{out}$ (19). However, in homozygous (*cir/cir*) mice, Cl^- accumulation through NKCC1 is obscure at ages over P9 because NKCC1 was not as active compared to heterozygous (+/*cir*) mice. The other possible candidate might be HCO_3^- because glycine receptors form ion channels which are not only permeable to Cl^-, but also to HCO_3^- (23). At a pH of 7.2, the $[HCO_3^-]$in would be near 16 mM, resulting in a HCO_3^- equilibrium potential of approximately -12 mV (24). Therefore, part of the depolarized E_{gly} might be explained by an efflux of HCO_3^-. In our recording conditions using bicarbonate as a buffer, we could not eliminate HCO_3^-, thus further study using bicarbonate-free conditions might be needed. We used the whole cell voltage clamp instead of the gramicidin-perforated technique, which has been frequently used to investigate the functions of KCC2 and NKCC1 in other studies (20, 25, 26). Despite whole-cell dialysis with internal pipette solution, our data showed changes in E_{gly} by the application of bumetanide or furosemide indicating that whole cell voltage clamp can be used for the functional analysis of KCC2 and NKCC1.

Thermodynamically, KCC2 can function as a Cl^- accumulator or extruder depending on the changes in the $[Cl^-]_{in}$ within the physiologic range. As the direction of the KCC2 transport is sensitive to small changes in the $[Cl^-]_{in}$ and $[K^+]_{out}$ near physiologic levels (19), the negative shifts of the E_{gly} induced by bumetanide in heterozygous (+/*cir*) or homozygous (*cir/cir*) mice might result from the inhibition of KCC2 alone because bumetanide is known to partially block KCC2 (22). However, this interpretation cannot stand in heterozygous (+/*cir*) mice because co-ad-

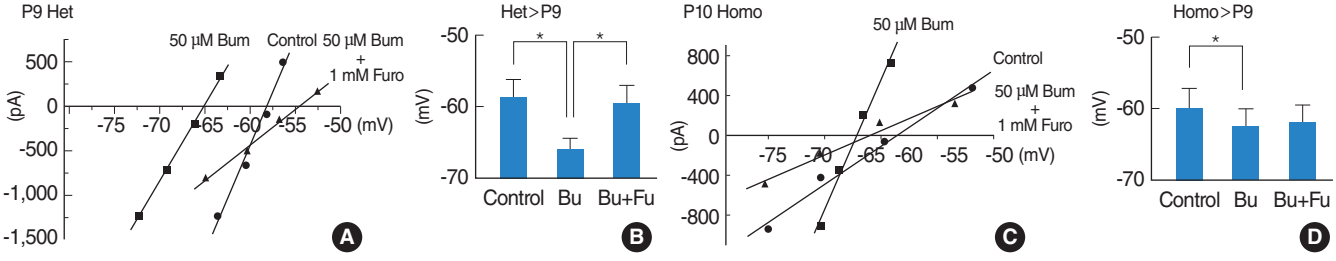

Fig. 4. The reversal potential of the glycine-evoked currents at different step potentials. The amplitudes of the currents obtained from P9–P12 heterozygous (Het) (+/*cir*) or homozygous (Homo) (*cir/cir*) were plotted as a function of corrected potentials (A, C). The solid lines through the symbols were obtained from a linear fit to the current amplitudes. Filled circles represent the data obtained from control condition, while filled squares and filled triangles present the data from 50 μM bumetanide (Bum) and 50 μM bumetanide plus 1 mM furosemide (Furo), respectively. The means of the E_{gly} with standard errors are presented in (B, D) with bar graphs. The statistical data were obtained from different mice groups (B, Het [+/*cir*] older than P9; D, Homo [*cir/cir*] older than P9). *The statistical significance ($P<0.05$).

ministration of furosemide and bumetanide shifted the E_{gly} to a less negative potential. If KCC2 were the only transporter influencing the E_{gly}, co-administration of furosemide with bumetanide would shift the E_{gly} to a more negative potential, which was not the case. Thus, it might be reasonable to suggest that the bumetanide-induced negative shift of the E_{gly} and its recovery by furosemide reflects the involvement of NKCC1 and KCC2 in the determination of the E_{gly} in heterozygous (+/*cir*) mice.

Functionally, the effect of bumetanide was weak and that of furosemide was statistically insignificant in homozygous (*cir*/*cir*) mice. The less potent effect of bumetanide or furosemide might be partially explained by the less prominent immunoreactivities of KCC2 and NKCC1 in homozygous (*cir*/*cir*) mice. However, less prominent immunoreactivity of KCC2 can not explain the nearly absence of effect of furosemide in homozygous (*cir*/*cir*) mice. Thus, some impaired function or delayed development of both transporters in homozygous (*cir*/*cir*) mice might be suggested.

Biochemical studies have demonstrated homo-oligomeric organizations of cation-chloride co-transporters (27, 28) and KCC2 is reported to developmentally change its form from monomers to oligomers (29). These studies raise the possibility that NKCC1 and KCC2 of homozygous (*cir*/*cir*) mice are developmentally immature to produce the similar responses found in heterozygous (+/*cir*) mice of the same age. The other possibility of impaired function has been reported in hypothyroid rats (23). In hypothyroid rats, glycine exerts a depolarizing effect on the E_{gly} until P11, almost 1 week longer than in control rats, in which a depolarizing-hyperpolarizing shift occurs at P5–P6. The immunohistochemical finding demonstrates an unchanged KCC2 distribution in hypothyroid rats compared to control rats, implying normal KCC2 gene expression, but impaired KCC2 function. In hypothyroid rats, some post-translational modification was suggested as a possible mechanism. Because we found equal or more prominent immunoreactivities of NMDA receptor subtypes in homozygous (*cir*/*cir*) than heterozygous (+/*cir*) mice (5), one of the possible mechanisms might be the down-regulation of KCC2 by Ca^{2+} influx through NMDA receptors, which was suggested in dissociated culture of mature hippocampal neurons (15). However, whether NKCC1 and KCC2 are developmentally immature or are modified by some post-translational mechanisms needs further study. The report that cochlear ablation abolished the expression of KCC2 mRNA in P14-P15 rat LSO (16) raises the other possibility of cochlear contribution to KCC2 or NKCC1 development; however, as cochlear hair cells are relatively intact at P10 (1), the generation of abnormal spontaneous activities from relatively intact hair cells should be proved to elucidate this point.

Our data suggest weak contributions of NKCC1 and KCC2 in the determination of the E_{gly} in homozygous (*cir*/*cir*) mice. Thus, the prolonged depolarizing phase might be possible in MNTB-LSO synapses of homozygous (*cir*/*cir*) mice, as was reported in experimentally hypothyroid rats (23). Generally, a depolarizing period and an elevation of $[Ca^{2+}]_{in}$ for its consequence is thought to provide a trophic signal for neuritogenesis (30), synapse formation (31, 32), and morphologic differentiation (33). Thus, future studies should be aimed at testing the actual presence of the depolarizing-hyperpolarizing shift of homozygous (*cir*/*cir*) LSO neurons and the relationship to the developmental changes of MNTB-LSO synapse formation.

CONFLICT OF INTEREST

No potential conflict of interest relevant to this article was reported.

ACKNOWLEDGMENT

This research was supported by the Basic Science Research Program through the National Research Foundation of Korea (NRF), funded by the Ministry of Education, Science and Technology (314-2008-1-E00151).

REFERENCES

1. Chung WH, Kim KR, Cho YS, Cho DY, Woo JH, Ryoo ZY, et al. Cochlear pathology of the circling mouse: a new mouse model of DFNB6. Acta Otolaryngol. 2007 Mar;127(3):244-51.
2. Lee JW, Lee EJ, Hong SH, Chung WH, Lee HT, Lee TW, et al. Circling mouse: possible animal model for deafness. Comp Med. 2001 Dec;51(6):550-4.
3. Lee JW, Ryoo ZY, Lee EJ, Hong SH, Chung WH, Lee HT, et al. Circling mouse, a spontaneous mutant in the inner ear. Exp Anim. 2002 Apr;51(2):167-71.
4. Gillespie DC, Kim G, Kandler K. Inhibitory synapses in the developing auditory system are glutamatergic. Nat Neurosci. 2005 Mar;8(3): 332-8.
5. Hong SH, Kim MJ, Ahn SC. Glutamatergic transmission is sustained at a later period of development of medial nucleus of the trapezoid body-lateral superior olive synapses in circling mice. J Neurosci. 2008 Nov 26;28(48):13003-7.
6. Chen G, Trombley PQ, van den Pol AN. Excitatory actions of GABA in developing rat hypothalamic neurones. J Physiol. 1996 Jul 15;494 (Pt 2):451-64.
7. Cherubini E, Rovira C, Gaiarsa JL, Corradetti R, Ben Ari Y. GABA mediated excitation in immature rat CA3 hippocampal neurons. Int J Dev Neurosci. 1990;8(4):481-90.
8. Luhmann HJ, Prince DA. Postnatal maturation of the GABAergic system in rat neocortex. J Neurophysiol. 1991 Feb;65(2):247-63.
9. Singer JH, Talley EM, Bayliss DA, Berger AJ. Development of glycinergic synaptic transmission to rat brain stem motoneurons. J Neurophysiol. 1998 Nov;80(5):2608-20.
10. Wu WL, Ziskind-Conhaim L, Sweet MA. Early development of glycine- and GABA-mediated synapses in rat spinal cord. J Neurosci. 1992 Oct;12(10):3935-45.

11. Kandler K, Friauf E. Development of glycinergic and glutamatergic synaptic transmission in the auditory brainstem of perinatal rats. J Neurosci. 1995 Oct;15(10):6890-904.
12. Lohrke S, Srinivasan G, Oberhofer M, Doncheva E, Friauf E. Shift from depolarizing to hyperpolarizing glycine action occurs at different perinatal ages in superior olivary complex nuclei. Eur J Neurosci. 2005 Dec;22(11):2708-22.
13. Plotkin MD, Snyder EY, Hebert SC, Delpire E. Expression of the Na-K-2Cl cotransporter is developmentally regulated in postnatal rat brains: a possible mechanism underlying GABA's excitatory role in immature brain. J Neurobiol. 1997 Nov 20;33(6):781-95.
14. Rivera C, Voipio J, Payne JA, Ruusuvuori E, Lahtinen H, Lamsa K, et al. The K+/Cl- co-transporter KCC2 renders GABA hyperpolarizing during neuronal maturation. Nature. 1999 Jan 21;397(6716):251-5.
15. Kitamura A, Ishibashi H, Watanabe M, Takatsuru Y, Brodwick M, Nabekura J. Sustained depolarizing shift of the GABA reversal potential by glutamate receptor activation in hippocampal neurons. Neurosci Res. 2008 Dec;62(4):270-7.
16. Shibata S, Kakazu Y, Okabe A, Fukuda A, Nabekura J. Experience-dependent changes in intracellular Cl- regulation in developing auditory neurons. Neurosci Res. 2004 Feb;48(2):211-20.
17. Fiumelli H, Woodin MA. Role of activity-dependent regulation of neuronal chloride homeostasis in development. Curr Opin Neurobiol. 2007 Feb;17(1):81-6.
18. Vale C, Schoorlemmer J, Sanes DH. Deafness disrupts chloride transporter function and inhibitory synaptic transmission. J Neurosci. 2003 Aug 20;23(20):7516-24.
19. DeFazio RA, Keros S, Quick MW, Hablitz JJ. Potassium-coupled chloride cotransport controls intracellular chloride in rat neocortical pyramidal neurons. J Neurosci. 2000 Nov 1;20(21):8069-76.
20. Balakrishnan V, Becker M, Lohrke S, Nothwang HG, Guresir E, Friauf E. Expression and function of chloride transporters during development of inhibitory neurotransmission in the auditory brainstem. J Neurosci. 2003 May 15;23(10):4134-45.
21. Russell JM. Sodium-potassium-chloride cotransport. Physiol Rev. 2000 Jan;80(1):211-76.
22. Payne JA. Functional characterization of the neuronal-specific K-Cl cotransporter: implications for [K+]o regulation. Am J Physiol. 1997 Nov;273(5 Pt 1):C1516-25.
23. Bormann J, Hamill OP, Sakmann B. Mechanism of anion permeation through channels gated by glycine and gamma-aminobutyric acid in mouse cultured spinal neurones. J Physiol. 1987 Apr;385: 243-86.
24. Backus KH, Deitmer JW, Friauf E. Glycine-activated currents are changed by coincident membrane depolarization in developing rat auditory brainstem neurones. J Physiol. 1998 Mar 15;507(Pt 3): 783-94.
25. Friauf E, Wenz M, Oberhofer M, Nothwang HG, Balakrishnan V, Knipper M, et al. Hypothyroidism impairs chloride homeostasis and onset of inhibitory neurotransmission in developing auditory brainstem and hippocampal neurons. Eur J Neurosci. 2008 Dec;28(12): 2371-80.
26. Kakazu Y, Akaike N, Komiyama S, Nabekura J. Regulation of intracellular chloride by cotransporters in developing lateral superior olive neurons. J Neurosci. 1999 Apr 15;19(8):2843-51.
27. de Jong JC, Willems PH, Mooren FJ, van den Heuvel LP, Knoers NV, Bindels RJ. The structural unit of the thiazide-sensitive NaCl cotransporter is a homodimer. J Biol Chem. 2003 Jul 4;278(27):24302-7.
28. Moore-Hoon ML, Turner RJ. The structural unit of the secretory Na+-K+-2Cl-cotransporter (NKCC1) is a homodimer. Biochemistry. 2000 Apr 4;39(13):3718-24.
29. Blaesse P, Guillemin I, Schindler J, Schweizer M, Delpire E, Khiroug L, et al. Oligomerization of KCC2 correlates with development of inhibitory neurotransmission. J Neurosci. 2006 Oct 11;26(41): 10407-19.
30. Maric D, Liu QY, Maric I, Chaudry S, Chang YH, Smith SV, et al. GABA expression dominates neuronal lineage progression in the embryonic rat neocortex and facilitates neurite outgrowth via GABA(A) autoreceptor/Cl- channels. J Neurosci. 2001 Apr 1;21(7):2343-60.
31. Ben-Ari Y, Khazipov R, Leinekugel X, Caillard O, Gaiarsa JL. GABAA, NMDA and AMPA receptors: a developmentally regulated 'ménage à trois'. Trends Neurosci. 1997 Nov;20(11):523-9.
32. Kirsch J, Betz H. Glycine-receptor activation is required for receptor clustering in spinal neurons. Nature. 1998 Apr 16;392(6677):717-20.
33. Ben-Ari Y, Tseeb V, Raggozzino D, Khazipov R, Gaiarsa JL. Gamma-Aminobutyric acid (GABA): a fast excitatory transmitter which may regulate the development of hippocampal neurones in early postnatal life. Prog Brain Res. 1994;102:261-73.